

Figure S1. (A) A simplified genetic pathway for germline sex determination in *C. elegans* (32). Arrows and barred lines indicate positive and negative regulation, respectively. (B) Germline phenotypes of *her-1(RNAi)* and *fem-3(RNAi)* animals. Gonad arms of adult hermaphrodites subjected to RNAi as indicated were dissected and stained with the anti-MSP antibody (green) and the anti-RME-2 antibody (red), shown as merged views (top). DAPI-stained views of the same gonad arms are also shown (bottom). Scale bars: 50 μ m. Note that *her-1(RNAi)* animals produced both sperm and oocytes, whereas *fem-3(RNAi)* animals produced only oocytes. (C) Specific downregulation of *Y14* and *mag-1* expression in RNAi animals, as confirmed by northern blot analysis. 40s rRNA was used as a loading control. (D) Western blot analysis of the TRA-2 ICD in lysates from control, *Y14(RNAi)*, *mag-1(RNAi)* and *tra-2(RNAi)* animals. FIB-1 was used as a loading control. The relative levels of the TRA-2 ICD normalized to FIB-1 are shown below.

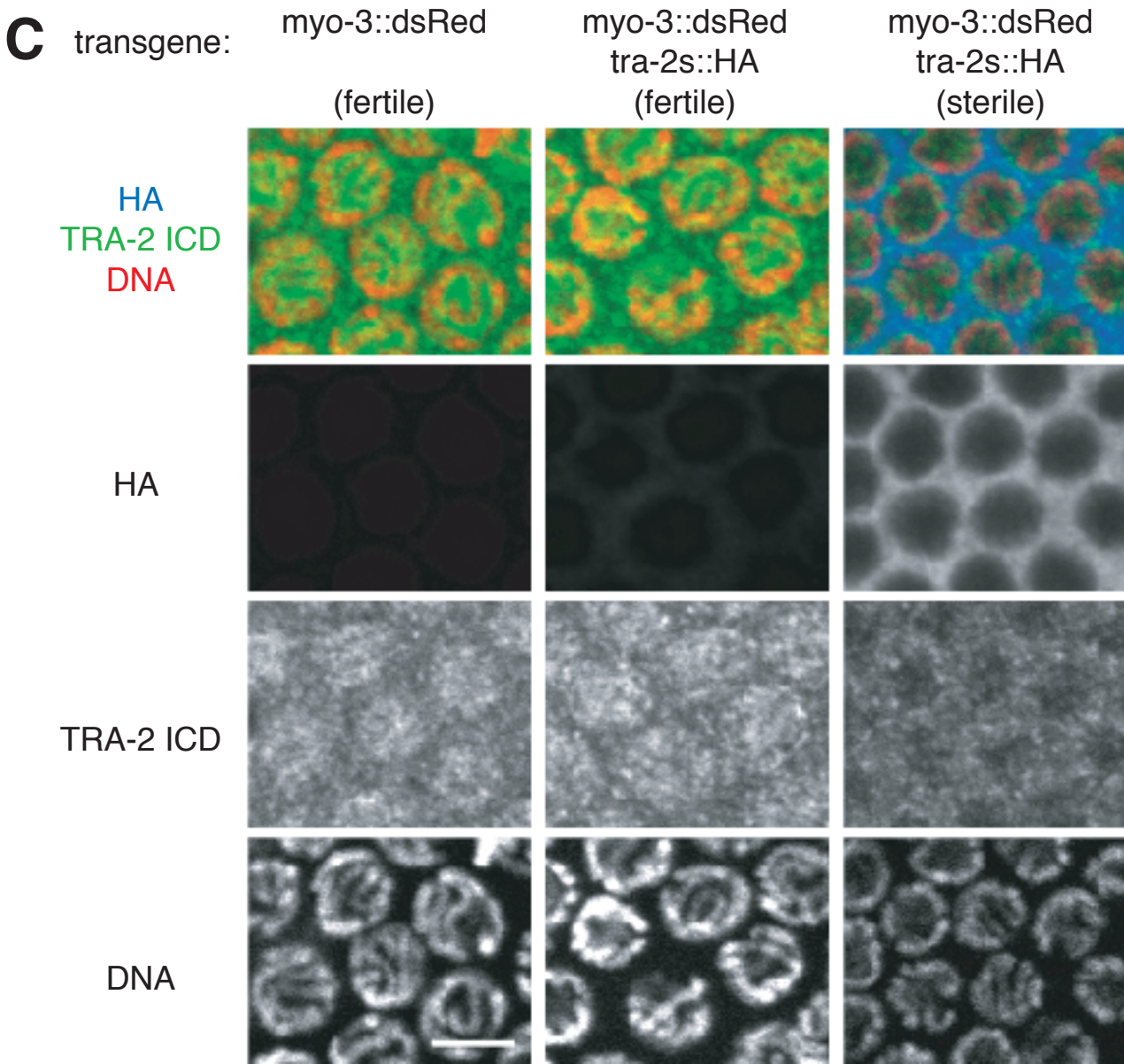
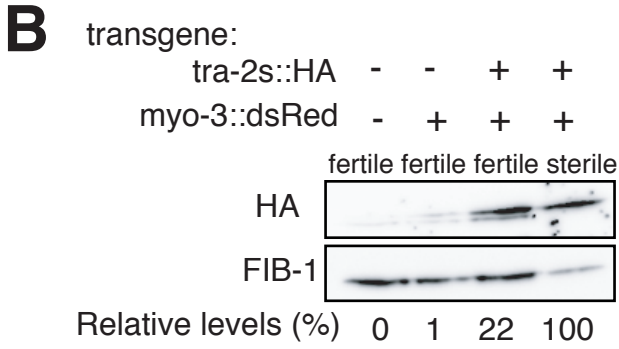
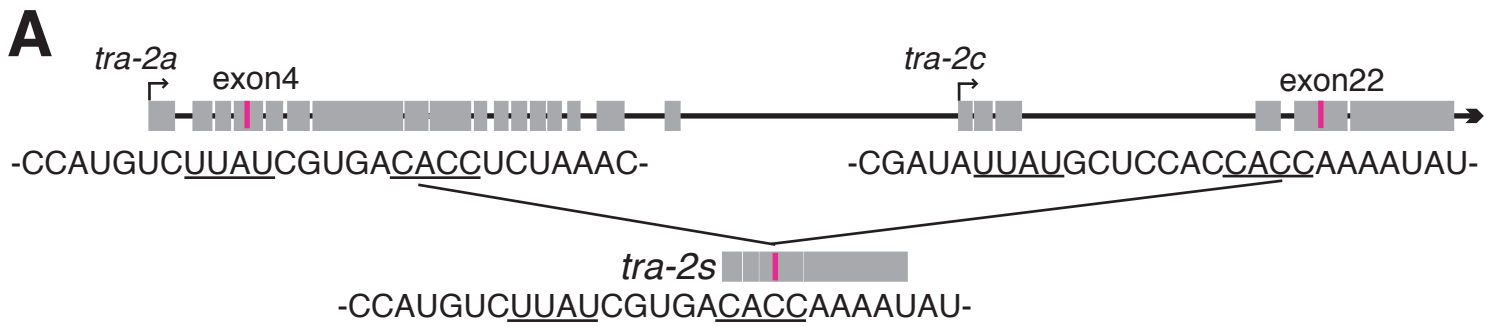


Figure S2. (A) Schematic representation of the exons and introns of the *tra-2* gene and *tra-2s* RNA. The splice donor and acceptor sites for the aberrant splicing that generates *tra-2s* RNA have bipartite direct repeat sequences, which are underlined in the diagram. (B) Expression of TRA-2S::HA in animals carrying the indicated transgenes. FIB-1 was used as a loading control. The relative levels of TRA-2S::HA normalized to FIB-1 are shown below. (C) Localization of TRA-2S::HA and its effect on the localization of the endogenous TRA-2 ICD. Germ cells in the pachytene stage within adult gonad arms of the indicated transgenic animals were stained with the anti-HA tag antibody (blue), anti-TRA-2 ICD antibody (green) and DAPI (red), shown as merged views (top). Separate views of the same cells are shown below. Scale bar: 4 μ m. Note that the endogenous TRA-2 ICD was not detectable in the nuclei of the sterile transgenic animal expressing high levels of TRA-2S::HA.

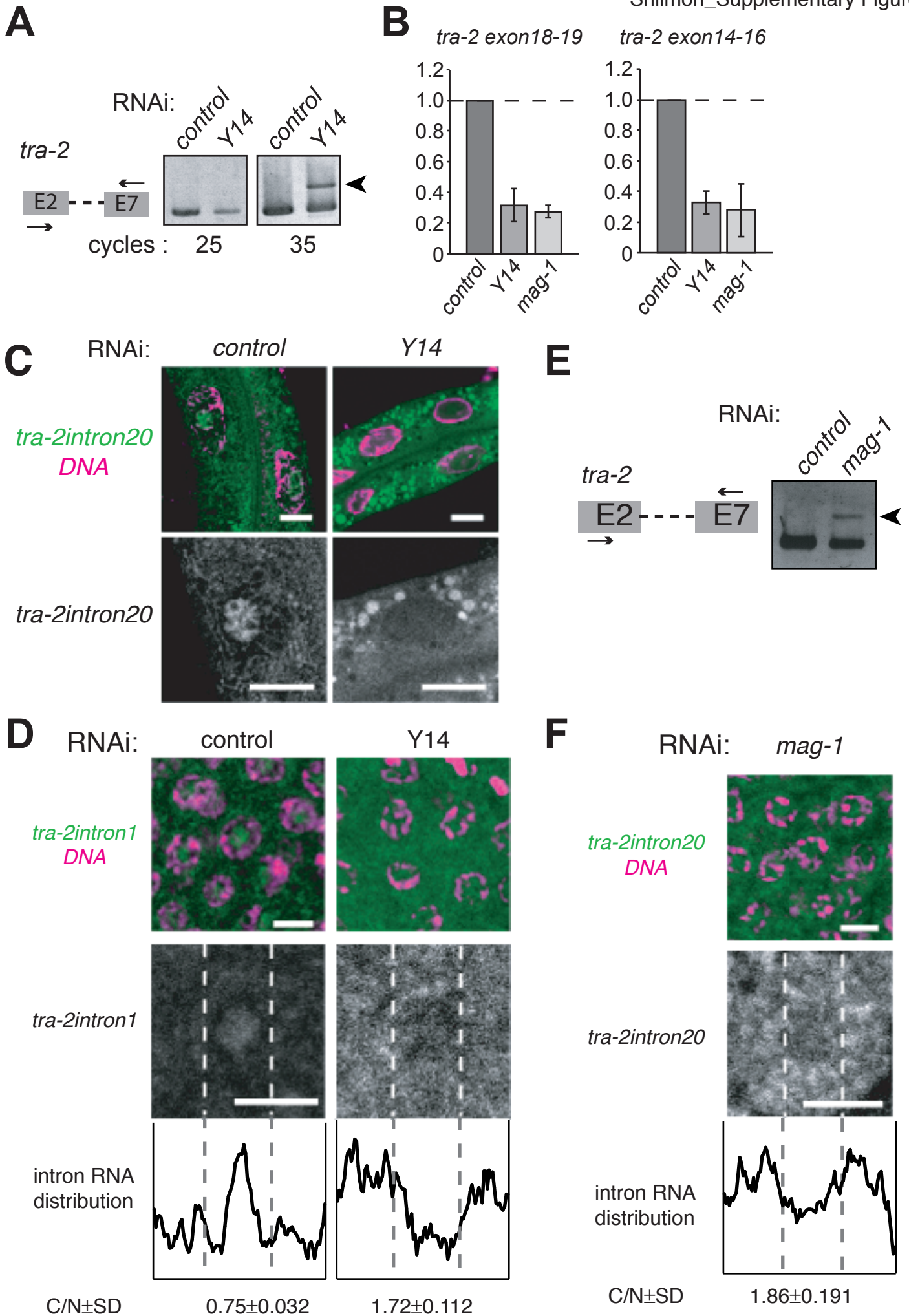


Figure S3. (A) RT-PCR assays were performed to monitor *tra-2* expression in *Y14(RNAi)* animals. The number of PCR cycles were indicated below. The primers used for amplification are schematically shown on the left. The arrow indicates unspliced *tra-2* RNA. (B) qRT-PCR assays were performed to monitor *tra-2* expression in *Y14(RNAi)* and *mag-1(RNAi)* animals. To see the expression levels of normal *tra-2* mRNAs, the relative amounts of *tra-2* RNAs containing exons 18-19 and exons 14-16 were measured. The relative values calculated from three independent experiments are shown with standard deviations. (C) *In situ* hybridization of intestinal cells in *Y14(RNAi)* animals. Cells were probed with *tra-2* intron 20 (green) followed by DNA staining (magenta), shown as merged views (top). Separate views probed with the intron are also shown (bottom). Scale bars: 8 μm . (D) *In situ* hybridization of mitotic cells within gonad arms dissected from *Y14(RNAi)* animals. Cells were probed with *tra-2* intron 1 (green) followed by DNA staining (magenta), shown as merged views (top). Separate views of single cells probed by the intron are also shown (middle). The intracellular distribution of the intron is shown as in Figure 3B (bottom). Scale bars: 4 μm . (E) RT-PCR assays were performed to monitor *tra-2* expression in *mag-1(RNAi)* animals. The primers used for amplification are schematically shown on the left. The arrow indicates unspliced *tra-2* RNA. (F) *In situ* hybridization of mitotic cells within gonad arms dissected from *mag-1(RNAi)* animals. Cells were probed with *tra-2* intron 20 (green) followed by DNA staining (magenta), shown as a merged view (top). Separate view of a single cell probed with the intron is also shown (middle). The intracellular distribution of the intron is shown as in Figure 3B (bottom). Scale bars: 4 μm .

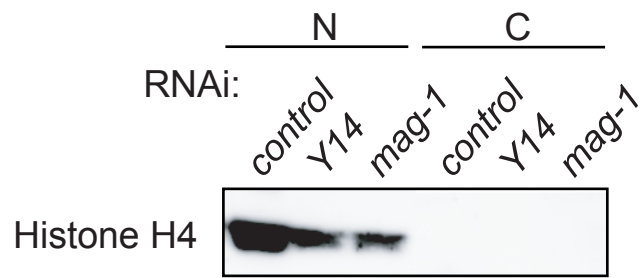
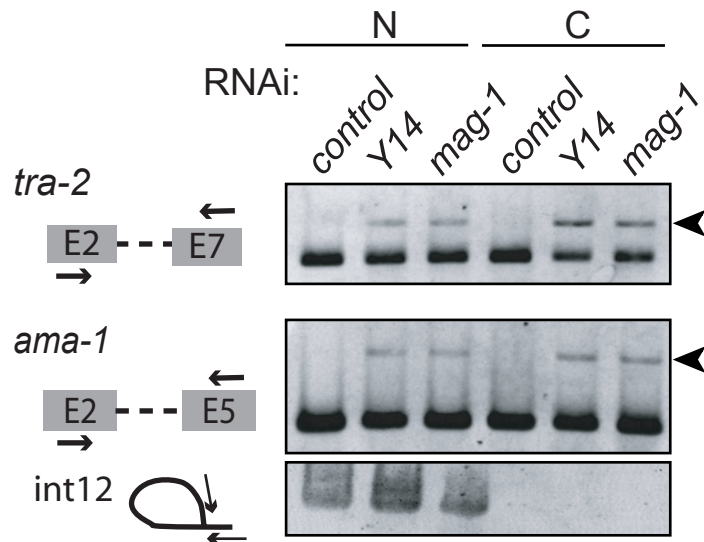
A**B**

Figure S4. (A) Western blot analysis of the histone H4 in the lysates of nuclear (N) and cytoplasmic (C) fractions prepared from the control, *Y14(RNAi)*, *mag-1(RNAi)* animals. Histone H4 was used as a marker for the nuclear fraction. (B) RT-PCR assays were performed to monitor the expression of *tra-2* and *ama-1* in nuclear (N) and cytoplasmic (C) fractions prepared from the same samples as used in (A). The primers used for amplification are schematically shown on the left. Arrowheads indicate unspliced RNAs.

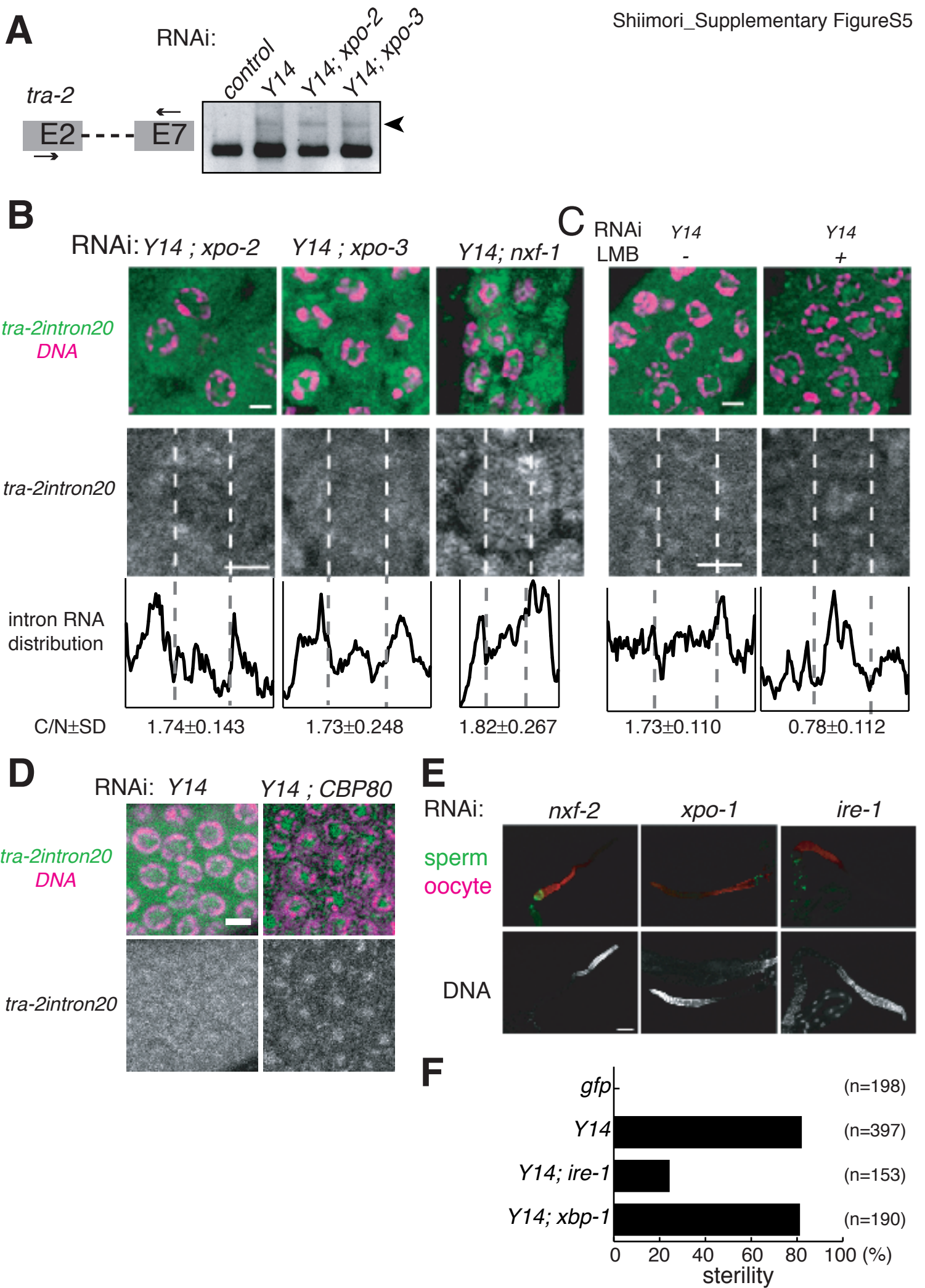


Figure S5. (A) RT-PCR analysis was performed to monitor *tra-2* expression in adult hermaphrodites subjected to RNAi as indicated. The primers used for amplification are schematically shown on the left. The arrowhead indicates unspliced *tra-2* RNA. (B) *In situ* hybridization of mitotic cells within gonad arms dissected from adult hermaphrodites subjected to RNAi as indicated. Cells were probed with *tra-2* intron 20 (green) followed by DNA staining (magenta), shown as merged views (top). Separate views of single cells probed with the intron are also shown (middle). Intracellular distribution of the introns is shown as in Figure 3B (bottom). Scale bars: 4 μm . (C) *In situ* hybridization of mitotic cells within gonad arms dissected from *Y14(RNAi)* animals with or without LMB treatment. Scale bars: 4 μm . (D) *In situ* hybridization of mitotic cells within gonad arms dissected from *Y14(RNAi)* and *Y14(RNAi);CBP80(RNAi)* animals. Cells were probed with *tra-2* intron 20 (green) followed by DNA staining (magenta), shown as merged views (top). Separate views probed with the intron are also shown (bottom). Scale bar: 4 μm . (E) Germline phenotypes of *nxf-2(RNAi)*, *xpo-1(RNAi)* and *ire-1(RNAi)* animals. Gonad arms were dissected and stained with the anti-MSP antibody (green) and the anti-RME-2 antibody (red), shown as merged views (top). DAPI-stained views of the same gonad arms are also shown (bottom). Scale bar: 50 μm . Note that these RNAi animals produced both sperm and oocytes. (F) Sterility caused by RNAi as indicated.

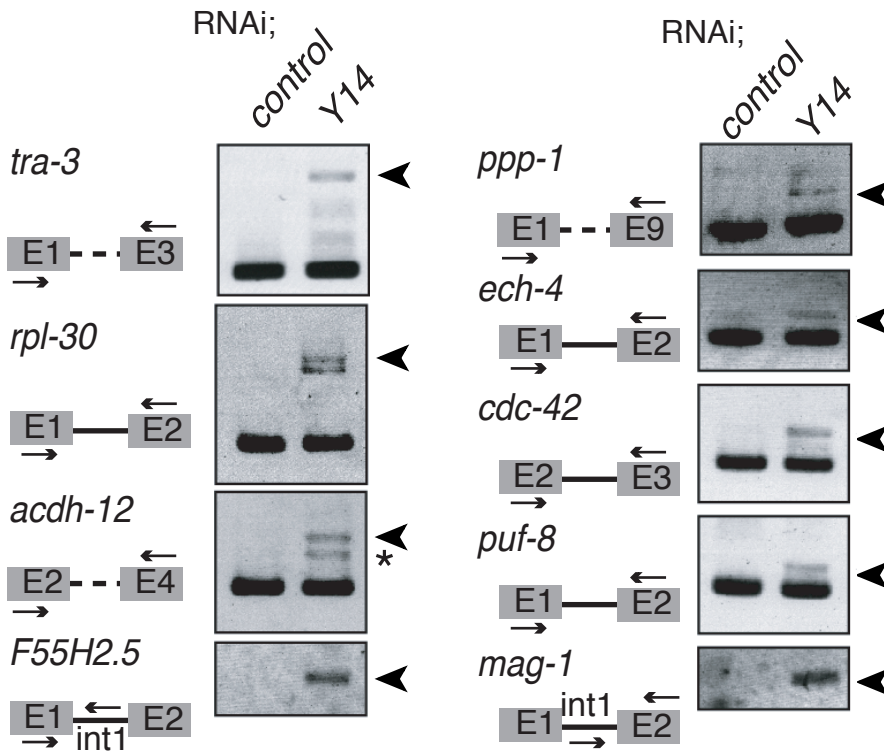


Figure S6. RT-PCR assays were performed to monitor the presence of unspliced RNAs in Y14(RNAi) animals. The primers used for amplification are schematically shown on the left. Arrowheads indicate unspliced RNAs. The asterisk indicates a non-specifically amplified product. Note that F55H2.5 and mag-1 are single intron-containing genes.

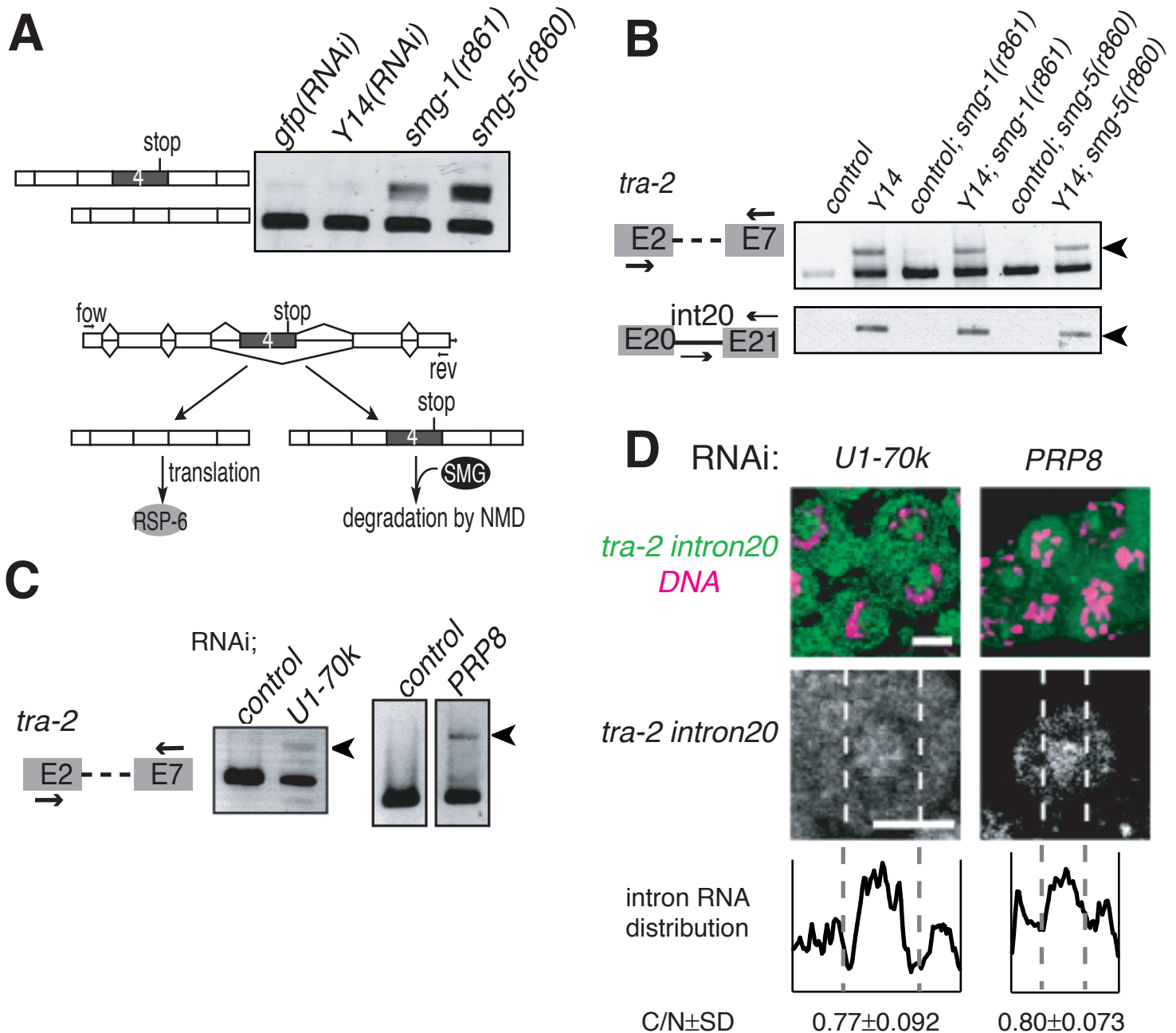


Figure S7. (A) RT-PCR assays were performed to monitor *rsp-6* expression in Y14(RNAi) animals and smg mutants deficient for NMD. *rsp-6* contains an alternatively spliced exon 4 that has a PTC. PTC-containing *rsp-6* mRNA is normally degraded by NMD. (B) RT-PCR assays were performed to monitor *tra-2* expression in Y14(RNAi) animals with or without the smg mutation background. The primers used for amplification are schematically shown on the left. Arrowheads indicate unspliced RNAs. (C) RT-PCR assays were performed to monitor *tra-2* expression in *U1-70k(RNAi)* and *PRP8(RNAi)* animals. (D) *In situ* hybridization of mitotic cells within gonad arms dissected from *U1-70k(RNAi)* and *PRP8(RNAi)* animals. Cells were probed with *tra-2 intron 20* (green) followed by DNA staining (magenta), shown as merged views (top). Separate views of single cells probed with the intron are also shown (middle). The intracellular distribution of the introns is shown as in Figure 3B (bottom). Scale bars: 4 μ m.

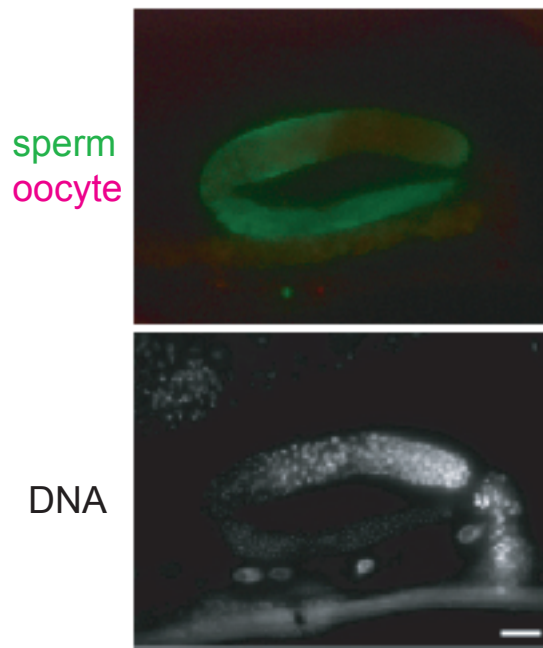
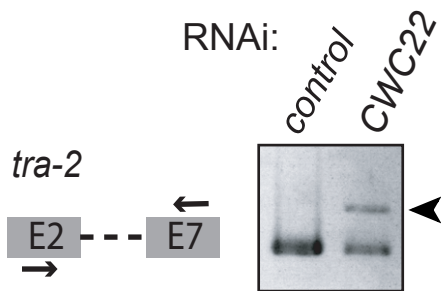
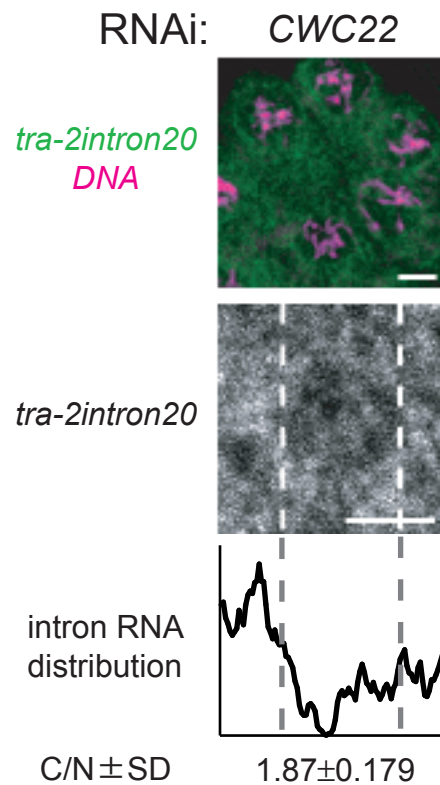
A*eIF4A3(RNAi); rrf-1(pk1417)***B***CWC22(RNAi); rrf-1(pk1417)***C****D**

Figure S8. (A, B) *eIF4AIII(RNAi)* and *CWC22(RNAi)* caused germline masculinization in the background of the *rrf-1* mutation. Gonad arms of *rrf-1(pk1417)* adult hermaphrodites subjected to RNAi as indicated were dissected and stained with the anti-MSP antibody (green) and the anti-RME-2 antibody (red), shown as a merged view (top). DAPI-stained view of the same gonad arm is shown (bottom). Asterisks indicate the distal end of the gonad. Note that expression of the oocyte marker was not detectable in these gonad arms. Scale bar: 50 μm in (A), 20 μm in (B). (C) RT-PCR assays were performed to monitor *tra-2* expression in *CWC22(RNAi)* animals. The primers used for amplification are schematically shown on the left. The arrow indicates unspliced *tra-2* RNA. (D) *In situ* hybridization of mitotic cells within the gonad arms dissected from *CWC22(RNAi)* animals. Cells were probed with *tra-2* intron 20 (green) followed by DNA staining (magenta), shown as merged views (top). Separate views of single cells probed by the intron are also shown (middle). The intracellular distribution of the intron is shown as in Figure 3B (bottom). Scale bars: 4 μm .

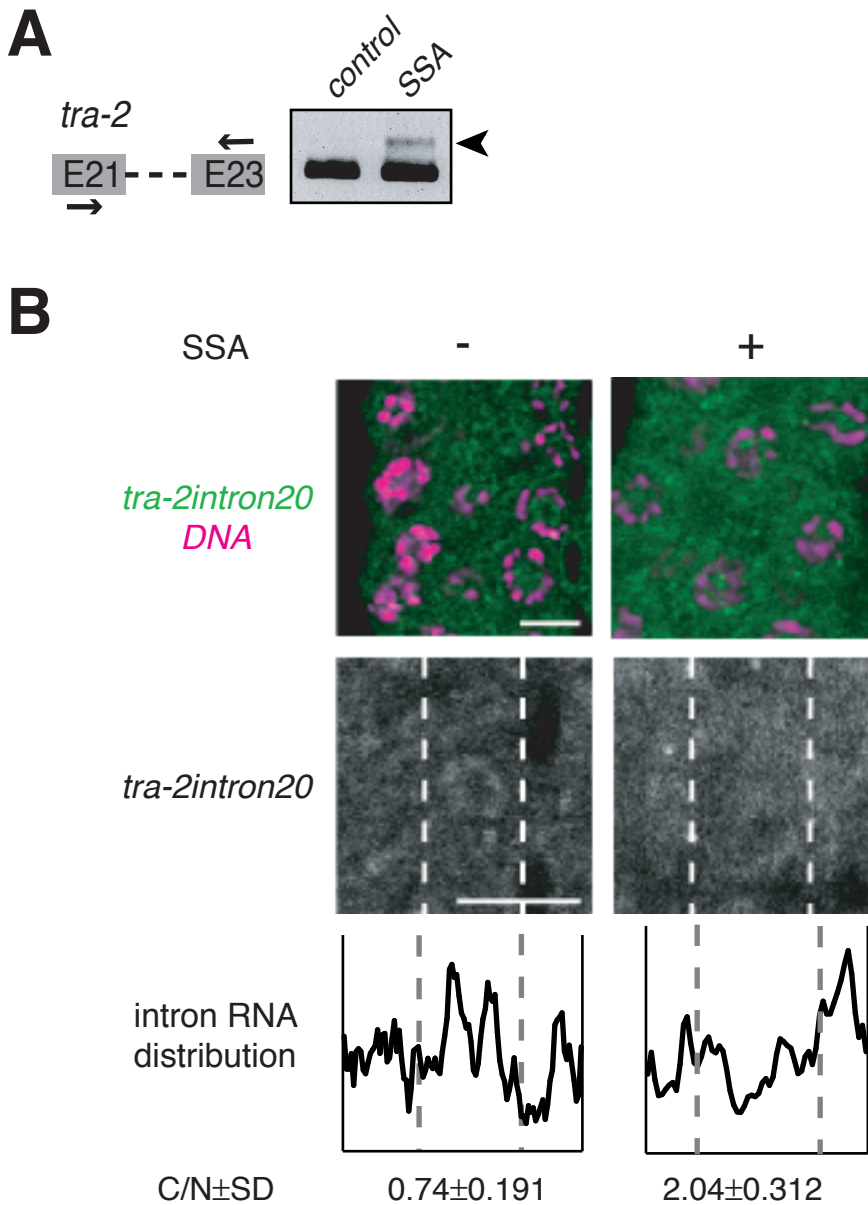


Figure S9. (A) RT-PCR analysis was performed to monitor *tra-2* expression in animals treated with spliceostatin A (SSA). The primers used for amplification are schematically shown on the left. The arrowhead indicates unspliced *tra-2* RNA. (B) In situ hybridization of mitotic cells within gonad arms dissected from animals with or without SSA treatment. Cells were probed with *tra-2* intron 20 (green) followed by DNA staining (magenta), shown as merged views (top). Separate views of single cells probed with the intron are also shown (middle). The intracellular distribution of the introns is shown as in Figure 3B (bottom). Scale bars: 4 μ m.

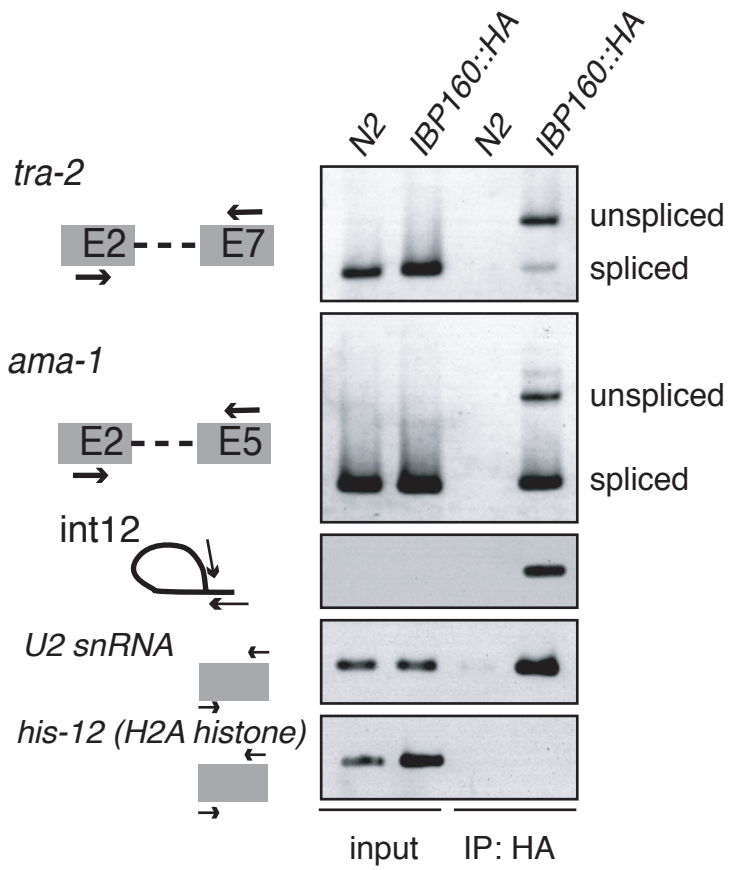


Figure S10. IBP160 associates with introns during pre-mRNA splicing in *C. elegans*. The lysate of the transgenic strain expressing HA-tagged IBP160 was immunoprecipitated using the anti-HA tag antibody. The precipitate was examined by RT-PCR. The primers used for amplification are schematically shown on the left. The wild type N2 strain was used as a control.

Table S1

gene	sequence	protein	masculization of germ line	other phenotype
<i>rnp-4</i>	R07E5.14	Y14	Yes	embryonic lethal, slow growth
<i>mag-1</i>	R09B3.5	Mago nashi	Yes	embryonic lethal, slow growth
-	F33D11.10	eIF4AIII	Yes*	sterile, embryonic lethal, larval arrest, Larval lethal
<i>hel-1</i>	C26D10.2	UAP56	N.D.	sterile, embryonic lethal, larval arrest, Larval lethal
<i>rnp-5</i>	K02F3.11	RNPS1	No	slow growth
<i>rsr-1</i>	F28D9.1	SRm160	No	WT
<i>aly-1</i>	C01F6.5	REF/Aly	No	WT
<i>aly-2</i>	F23B2.6	REF/Aly	No	WT
<i>aly-3</i>	M18.7	REF/Aly	No	WT
<i>smg-4</i>	F46B6.3	Upf3	No	WT
-	W08E3.2	MLN51/BTZ	No	WT
-	T20G5.9	PYM	No	embryonic lethal, slow growth

Table S1. Phenotypes resulting from RNAi of the EJC subunits. Injection RNAi and L1 soaking RNAi were performed using the wild type N2 strain, except when the germline effect of *eIF4AIII*(RNAi) was examined*, in which *rrf-1(pk1417)* was used to avoid pleiotropic somatic phenotypes (see Supplementary Figure S7).

Table S2. Primer list

target gene	Direction	sequence (5'-3')
tra-2 exon2-exon7	forward	AACTGCAGCCATCGTTTGTAGCCAGGG
tra-2 exon2-exon7	reverse	TAGGATCCCTTGATCATCCACACAATCG
tra-2 exon21-exon-23	forward	AACTGCAGATCATCTGCTCCATCGTTCCCG
tra-2 exon21-exon-23	reverse	CGGGATCCCGAGATTCCCTTCTCTGTGCCG
tra-2 intron20-exon21	forward	AACTGCAGTAGTGTCTCGACATGGTGGC
tra-2 intron20-exon21	reverse	AACTGCAGGAGGATTACTGTAGGTACG
ama-1	forward	GGGATATCTCCAGAAGTCTACGAGAACGG
ama-1	reverse	AACTGCAGACACGGCGGTATGATGGTTG
ama-1 intron12-exon13	forward	CCGCTCGAGTACACTCCATCCTCGCCG
ama-1 intron12-exon13	reverse	CGGGATCCGTTTGTCCGTAACCTTTCG
ife-4	forward	CCGCTCGAGGCTGAAACGTCAACTCAGG
ife-4	reverse	AACTGCAGGGCCGTTTGAAATGCACC
tra-3	forward	CCGCTCGAGTTTGTGTCTGCCTGCTCCGCC
tra-3	reverse	AACTGCAGTGTACGTGCTGCAATGGCAGCC
rsp-6	forward	CCGCTCGAGGGACGCCAAGGTGTACGTCGG
rsp-6	reverse	GGAATTCTTAGTGCGGAGAAGCAGAACGGC
ppp-1	forward	AACTGCAGATGCACGAAATGCAAGGG
ppp-1	reverse	ACGGATCCTTAATCATCGGTCCATTCTTCG
clec-87	forward	CCGCTCGAGGTTCAAGCCAAGGAAGCC
clec-87	reverse	CGGGATCCCGATTCCAGGGATGATGG
acdh-12	forward	AACTGCAGTCCGCCTCTCATTGCTC
acdh-12	reverse	CGGGATCCGGCAACACGGTGCATCTC
rpl-30	forward	CCGCTCGAGATGGCTCCAGCTGCTAAGC
rpl-30	reverse	CGGGATCCACAAGCTTAGCCTTCCG
ech-4	forward	CCGCTCGAGTCGAAATCTCACCTCGC
ech-4	reverse	CGGGATCCCATCCTGAGTTGTCCC
cdc-42	forward	AACTGCAGCAGTAATGATCGGTGGCG
cdc-42	reverse	CGGGATCCACTTCTCTCCAACATCCG
puf-8	forward	AACTGCAGGGAGATGCGTTGGCTGTC
puf-8	reverse	CGGGATTCTCTTCTCGAGCCACATGC
U1 snRNA	forward	GGAATTCAAACCTTACCTGGCTGGGG
U1 snRNA	reverse	CGGGATCCTTCAGGGCCGCGCGCACG
U2 snRNA	forward	CCGCTCGAGATCGCTTCTTCGGCTTATTAG
U2 snRNA	reverse	GGAATTCCTGGGCCGAGCCCGGCAG
U4 snRNA	forward	CCGCTCGAGAGCTTTGCGCTGGGGCG
U4 snRNA	reverse	GGAATTCTTCTGCCTCCTGGAGGCG
U5 snRNA	forward	CCGCTCGAGAACTCTGGTTCCTCTGC
U5 snRNA	reverse	GGAATTCTGTCCCGCTTCTCAAGG
U6 snRNA	forward	CCGCTCGAGGTTCTTCCGAGAACATATAC
U6 snRNA	reverse	GGAATTCAAAATTTGGAACGCTTCACG
ama-1 lariat intron	forward	AACTGCAGCCAGAAATTAGGCGCTTACTG
ama-1 lariat intron	reverse	CGGGATCCTGCACTTTTTTCATGTTTTCTCG
ama-1 lariat intron	forward	AACTGCAGTGAAAATTTGGTGAAAATTACGG
ama-1 lariat intron	reverse	CGGGATCCCGACCAAATAACAGATTTTCCA
his-12	forward	AACTGCAGATGTCTGGACGTGGAAAGG
his-12	reverse	CGGGATCCCTATTCTTATCTCCACCG
tra-2 exon18-19	forward	CTCACTACAGCAGGGATCTTCA
tra-2 exon18-19	reverse	CCCAACGACCAATAAGGAAA
tra-2 exon14-16	forward	TCTGAAGCAGTTCAGTGAGGAC
tra-2 exon14-16	reverse	TCTGCAGAAGCATTCTATTAGTTTC
rpl-4	forward	AAAGCTCCGCAACCGTCAA
rpl-4	reverse	GCACTCAGCATCTGTCCGTAG